



Drag Reduction Through Employing Leading-Edge Tubercle on The Airfoil

Intizar Ali^{1,2*}, Tanweer Hussain², Ali Akbar Shah Syed¹, Danish Inam¹, Syed Muhammad Kashif Shah¹, Inam Ul Ahad¹

¹I-Form, the SFI Research Centre for Advanced Manufacturing, School of Mechanical & Manufacturing Engineering, Dublin City University, Dublin, Ireland

²Department of Mechanical Engineering, Mehran UET Jamshoro Sindh, Pakistan

Intizar.ali@dcu.ie

Abstract. Drag reduction over the lifting surfaces has remained a key interest of aerodynamic researchers over the last five decades, due to rising fossil fuel prices, global warming and climate change. The drag over the lifting surfaces is closely related to the required thrust and consumption of fossil fuels thus overall emissions. In this connection, the present study aims to analyze the drag performance of leading-edge tubercle airfoil in pre- and post-stall regimes. For that purpose, two wing models, one with a smooth leading edge and the second with a tubercle leading edge were designed and simulated. The computational fluid dynamics CFD simulation was performed in a transitional flow regime. The wing model was developed by using the NACA0021 airfoil profile and simulated at chord-based Reynolds number of $Re_c=2.4 \times 10^5$. The numerical simulation results reveal that tubercles at the leading edge have a favorable effect on airfoil drag performance. It was found that at a lower angle of attack portion of viscous drag is very close to the pressure drag acting on the airfoil. However, at higher angles of attack contribution of viscous drag in total drag is reduced to about 5- 10%. It was also observed that at higher angles of attack viscous drag over tubercle leading edge airfoil is higher than the viscous drag of the baseline airfoil model, due to attached flow.

Keywords: Drag reduction, Leading edge tubercle, airfoil, Reynolds number; angle of attack; Stall delay; Flow Separation control

1 Introduction

Drag reduction and flow separation control has remained main interest of aerodynamic research just after 1973 oil crises. Further during recent year's significant rise in air transport, climate change and rising prices of fossil fuels thrusts aerodynamic scientists to look for greener aircrafts. Thus in order to meet energy requirements and design efficient machines numerous funding is devoted to design efficient turbines, compressors, aircrafts and ships. As part of this research marine biologist's analyzed connection between external design, aquatic animal surface finish and swimming behaviour of various aquatic animals. They have found that the hydrodynamic effectiveness of the humpback whale flipper is enhanced by tubercles located at its Leading Edge (LE) [1], as they investigate the morphologies of many aquatic creatures. Tubercles near the flipper's LE have been seen to potential to delay stall, maintain high lift at higher angle of attack and enhance maneuverability. Research has indicated that LE tubercles may find use in wind turbines [2–6], hydroplanes, rudders, propellers, and helicopters (for reducing dynamic stall). Additionally, LE tubercles are used in a variety of

© The Author(s) 2024

I. U. Ahad (ed.), *Proceedings of the 4th International Conference on Key Enabling Technologies (KEYTECH 2024)*, Atlantis Highlights in Engineering 35,
https://doi.org/10.2991/978-94-6463-602-4_16

engineering devices, including the inverted wing on race car decks, which improve handling performance [7, 8], compressor and fan blades, which improve fatigue life by controlling stall, and wind turbine blades, fans, and compressors [9–12], which reduce tonal noise. The main issue with LE tubercles, however, is that they improve wing performance in the post-stall regime at the expense of wing performance deteriorating in the pre-stall regime [6, 10, 13–17], which has limited the practical uses of LE tubercles. Moreover, very limited studies have focused on detailed drag performance of tubercle wing models.

2 Numerical simulation

2.1 Modeling & Meshing

The wing models were designed by using NACA0021 airfoil profile, where the coordinates of airfoil profile were obtained from University of Illinois Urbana-Champaign website. Moreover, the two wing models, one with smooth leading edge and second with tubercle leading edge were developed. The wing models were developed with mean chord of 70 mm and span length of 69.3 mm. Moreover, the NACA0021 airfoil is selected because it has significant resemblance with humpback whale profile. The tubercle wing model is produced through applying coordinate transformation equation (1). Moreover, the amplitude of the leading tubercle is 3% of chord where the wavelength of the tubercle is 11% of the chord. Both wing models were developed in Pro-Engineer software, initially 2D airfoil profile is generated from the coordinates. The wing model is produced by using a 2D airfoil profile. Moreover, numerous research studies used NACA0021 airfoil profile to analyze the impact of employing tubercles on the airfoil aerodynamic performance [1-5].

$$x = c + A \sin \left[2\pi \left(\frac{z}{\lambda} - \frac{\lambda}{2c} \right) \right] \quad (1)$$

The designed wing models are presented in Fig. 1 (a & b), the models were named as in quite simple way such as smooth leading edge (Baseline or base) and tubercle Leading edge wing model as (as tubercle LE). Once the 3D wing models were developed and imported in ANSYS design modeler then fluid domain is created around the wing model and wing model is rotated from 0° to 20° with the interval of 4°. The fluid domain along with applied boundary conditions at inlet, outlet, side walls and upper and bottom wall is presented in Fig. 1(c). The fluid domain is discretized where tetrahedral mesh elements were used and non-uniform mesh is generated. The fine mesh is generated near the airfoil surface through employing sphere of influence method where element size is 1.3mm and mesh airfoil surface is further refined through applying inflation layer to have closer look on the fluid parameter within the boundary layer. Furthermore, the growth ratio ≈ 1.1 is used to generate unstructured mesh around the wing model; the mesh contains the total number of cells 2.6×10^7 . Since CFD employee finite volume method thus it is better to mention control volumes rather than discussing number of elements and nodes. Moreover, for predicting flow behavior accurately near the wing wall the inflation is applied in the close vicinity of the solid wing surface. The distance of the first layer from the wing surface is set at 0.053mm, thus ($Y^+ < 1$). The grid independence test is performed but not included in results because of pages limitation, for further details on GIT and validation of CFD model readers may refer to read [6]. The meshed model of the computational domain is presented in Fig. 1(d).

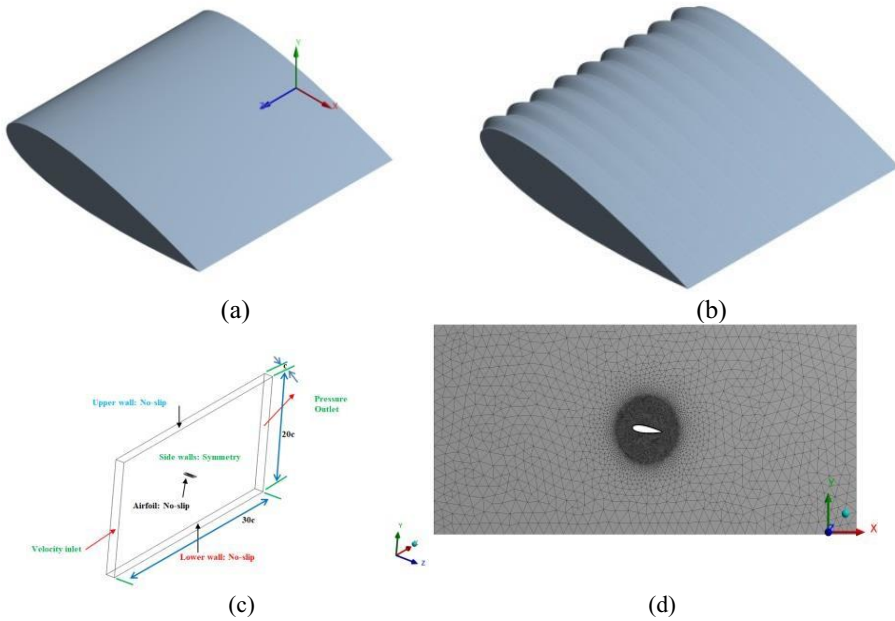


Fig. 01. The designed CAD model (a) the isometric view of the baseline wing (b) the isometric view of tubercle leading edge wing (c) Fluid domain along with applied boundary conditions (d) Meshed model of the fluid domain showing fine mesh within sphere of influence and layers of inflation applied over airfoil surface

2.2 Computational Set-up & Boundary conditions

In this research workflow over the airfoil is considered as viscous and incompressible because of it is low freestream Mach number. Thus, only continuity and momentum equation were solved through employing pressure-based solver. Flow is considered steady at lower angles of attack i.e. till 12° , however at 16° & 20° angle of attack flow is considered as unsteady. The convergence criteria for all the variables were set as 0.00001 which is analogues to number of studies [7]. Semi-Implicit method for pressure linked equations (SIMPLE) is used for pressure velocity coupling. Moreover, in case of unsteady simulation at higher angles of attack 0.0001 times step is used where 50 iteration was carried out in each time step. The inlet is defined as velocity inlet, where outlet is the pressure outlet. Moreover, the no-slip condition is applied on the airfoil wall. The symmetry boundary condition is applied on the fluid domain walls in spanwise direction. The detailed boundary conditions and the fluid domain are presented in Fig. 1(c).

3 Results & Discussion

Impact of employing leading edge tubercles on drag coefficient of the airfoil, is presented and discussed. The drag coefficient for smooth leading edge and tubercle LE wing model is plotted against the tested angles of attack. From Fig. 2 it is observed that tubercle airfoil experience lower drag as compared to smooth LE airfoil at all tested angles of attack. It can also be noticed that drag is quite low till 12° angle of attack; however, after that drag coefficient significantly increased due to stall i.e. massive flow separation. However, the difference of

drag coefficient is quite low at lower angles of attack. Moreover, at high angles attack i.e. at 16o and 20o angles of attack significant difference in drag coefficient is observed. It is estimated that maximum reduction in drag coefficient of about 8.3% and 17.7% is achieved at 8o and 20o angle of attack respectively, through employing tubercles at the leading edge of the airfoil. A detailed drag analysis regarding the contribution of each drag component is presented next section.

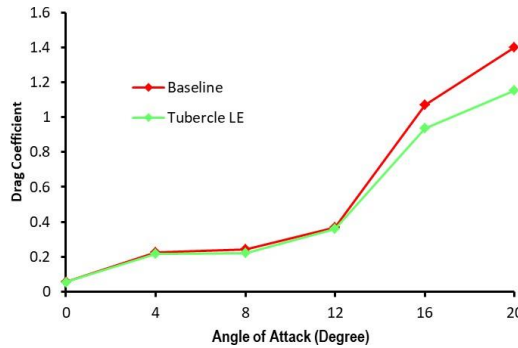


Fig. 2. The variation of Drag coefficient (CD) of the baseline and leading-edge tubercle airfoil against angle of attacks

3.1 Pressure Distribution

The pressure coefficient variation is presented and discussed in this section over the baseline and tubercle leading edge wing model at 8o and 20o angle of attack. From pressure distribution over the baseline wing model it is noticed leading edge suction is constant over the entire span length of the airfoil and adverse pressure gradient appears along the chord and pressure significantly increased near the trailing edge. However, in case of tubercle wing model strong leading-edge suction occurs at the trough of the tubercle, moreover it is clear from the pressure coefficient variation it is hypothesized that at tubercle peak fluid particles diverted towards trough causing strong suction at tubercle trough. Moreover, at 20o angle of attack in Fig. 3 (c & d) similar behavior of pressure coefficient variation is observed. However, in case baseline airfoil pressure over the airfoil is high on suction side as compared to the pressure on suction side of the leading-edge tubercle airfoil.

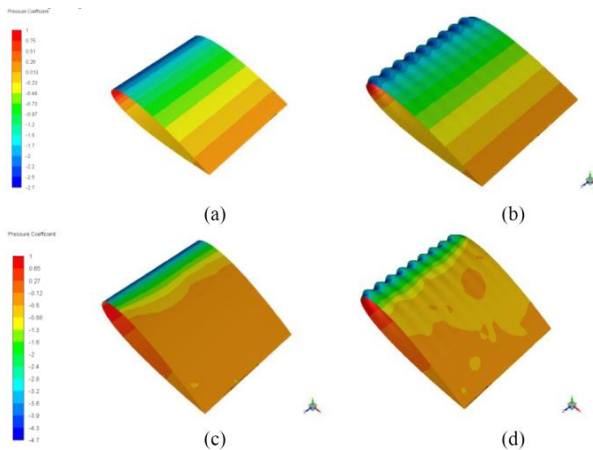


Fig. 3: Pressure coefficient distribution over (a) baseline wing showing smooth leading edge suction Tubercle leading edge wing model at 8o angle of attack (c) baseline wing model (d) Tubercle leading edge wing model at 20o angle of attack

To further understand the drag performance and flow mechanism, streamwise Wall Shear Stress (WSS) distribution over the baseline and tubercle LE airfoil is presented at 8o and 20o angle of attack. In streamline WSS the negative value of wall shear represents region of separated flow. At 8o angle of attack a very small region of negative WSS is noticed for baseline and tubercle LE wing model however, in case of baseline wing model there is no serration like behavior is noticed. Moreover, from at 20o angle of attack significant region of negative streamwise wall shear is noticed over baseline wing model, negative WSS were also noticed in case of tubercle wing model, but it is small as compared to baseline wing model. Thus, it is concluded that tubercles restrict flow separation, this in turn reduces drag of tubercle wing model. Similar assertion has been made by numerous studies, thus the flow behavior results are in close agreement with literature results [3, 4, 8-11].

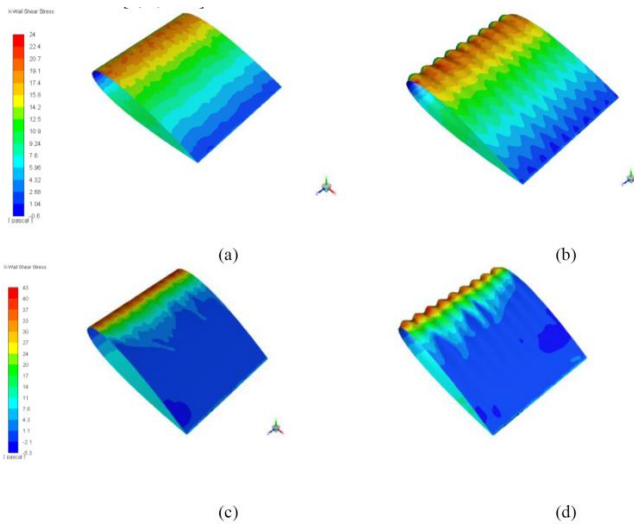


Fig. 4. Streamwise wall shear stress distribution over (a) baseline wing showing smooth leading-edge suction (b) Tubercle leading edge wing model at 8° angle of attack (c) baseline wing model (d) Tubercle leading edge wing model at 20° angle of attack

4 Conclusion

Present study aims at analyzing the impact of leading edge tubercles on the drag performance of the airfoil at chord based Reynolds number of $Re_c=2.4 \times 10^5$. CFD simulation performed in pre and post stall regime through considering the flow over the airfoil surface as viscous and incompressible. To analyze the effect of tubercle on airfoil drag, two wing models were developed one with smooth leading edge and second with tubercle LE. Numerical simulation results reveal that tubercles have favorable effect on the airfoil drag performance. It is also found that for both the airfoil contribution of pressure drag is significantly higher as compared to viscous drag. It is estimated that maximum reduction in drag coefficient of about 8.3% and 17.7% is achieved at 8o and 20o angle of attack respectively, through employing tubercles at the leading edge of the airfoil. It was found that at a lower angle of attack portion of viscous drag is very close to the pressure drag acting on the airfoil. However, at higher angles of

attack contribution of viscous drag in total drag is reduced to about 5-10%. The drag reduction in case of tubercle leading edge airfoil is associated with restriction of flow separation over the airfoil surface as compared baseline airfoil. It was also observed that at higher angles of attack viscous drag over tubercle leading edge airfoil is higher than the viscous drag of the baseline airfoil model, due to attached flow.

5 References

1. K. L. Hansen, R. M. Kelso, and B. B. Dally, "Performance variations of leading-edge tubercles for distinct airfoil profiles," *AIAA journal*, vol. 49, pp. 185-194, 2011.
2. R. Pérez-Torró and J. W. Kim, "A large-eddy simulation on a deep-stalled aerofoil with a wavy leading edge," *Journal of Fluid Mechanics*, vol. 813, pp. 23-52, 2017.
3. Skillen, A. Revell, A. Pinelli, U. Piomelli, and J. Favier, "Flow over a wing with leading-edge undulations," *Aiaa Journal*, vol. 53, pp. 464-472, 2015.
4. Tunio, D. Kumar, T. Hussain, and M. Jatoi, "Investigation of variable spanwise waviness wavelength effect on wing aerodynamic performance," *Fluid Dynamics*, vol. 55, pp. 657-669, 2020.
5. M. Zhao, Y. Zhao, Z. Liu, and J. Du, "Proper orthogonal decomposition analysis of flow characteristics of an airfoil with leading edge protuberances," *AIAA Journal*, vol. 57, pp. 2710-2721, 2019.
6. Ali, T. Hussain, I. N. Unar, L. Kumar, and I. U. Ahad, "Turbulence Model Study for aerodynamic analysis of the leading edge tubercle wing for Low Reynolds Number flows," *Heliyon*, 2024.
7. Hansen, R. Kelso, and B. Dally, "An investigation of three-dimensional effects on the performance of tubercles at low Reynolds numbers," in *17th Australasian Fluid Mechanics Conference*, Auckland, New Zealand, 2010, pp. 5-9.
8. Favier, A. Pinelli, and U. Piomelli, "Control of the separated flow around an airfoil using a wavy leading edge inspired by humpback whale flippers," *Comptes Rendus Mecanique*, vol. 340, pp. 107-114, 2012.
9. Zhao, M. Zhang, and J. Xu, "Numerical simulation of flow characteristics behind the aerodynamic performances on an airfoil with leading edge protuberances," *Engineering Applications of Computational Fluid Mechanics*, vol. 11, pp. 193-209, 2017.
10. Ali, T. Hussain, I. N. Unar, and M. Waqas, "Aerodynamic performance analysis of the wavy wing with varying spanwise waviness characteristics," *Bulletin of the American Physical Society*, 2022.
11. P. Yang, Y. Zhu, and J. Wang, "Effect of leading-edge tubercles on the flow over low- aspect-ratio wings at low Reynolds number," *Theoretical and Applied Mechanics Letters*, vol. 13, p. 100386, 2023.

Open Access This chapter is licensed under the terms of the Creative Commons Attribution-NonCommercial 4.0 International License (<http://creativecommons.org/licenses/by-nc/4.0/>), which permits any noncommercial use, sharing, adaptation, distribution and reproduction in any medium or format, as long as you give appropriate credit to the original author(s) and the source, provide a link to the Creative Commons license and indicate if changes were made.

The images or other third party material in this chapter are included in the chapter's Creative Commons license, unless indicated otherwise in a credit line to the material. If material is not included in the chapter's Creative Commons license and your intended use is not permitted by statutory regulation or exceeds the permitted use, you will need to obtain permission directly from the copyright holder.

